Quantum half-adder

Geraldo A. Barbosa*
Center for Photonic Communication and Computing, ECE Department, Northwestern University, 2145 North Sheridan Road, Evanston, Illinois 60208-3118, USA
(Received 13 April 2005; revised manuscript received 16 February 2006; published 26 May 2006)

Implementation of a linear optics quantum multibit half-adder that could show potential scalability is discussed. Parametric down-conversion sources are assumed that are pumped by a mode carrying orbital angular momentum l. A *single* photon from a pair is prepared by detection of its twin. This preparation of a single photon defines *two* bits to be summed *and* the starting *carry* control bit. This hyperentangled single photon enters a sequence of optical gates that acts on this photon and ancilla photons. At the adder output, each single photon detected gives the *sum* operation plus *carry*. The photons belong to a hyperentangled system with a 2^3 Hilbert space describing each photon. Conditions to have a scalable system for quantum computation define the requirements for construction of this photon source.

DOI: 10.1103/PhysRevA.73.052321 PACS number(s): 03.67.Lx, 42.50.−p, 42.65.Lm

I. INTRODUCTION

Quantum computation (QC) is a subject of intense theoretical and experimental research nowadays [1]. Difficult steps [2,3] are being taken to produce qubits and very modest gates. Ingenuity and state-of-the-art technology follow such difficult advances. Scalability has yet to be practically demonstrated, even for physical systems possessing a long interaction range. Photon systems add another complexity level due to the linear aspects of optics (nonexistence of interaction potential between photons in vacuum—at least in the desired energy range). The Knill, Laflamme, Milburn (KLM) scheme [4] proposes a way to implement efficient QC using only passive optics, photodetectors and single-photon sources. In the KLM scheme sign flips, for example, are obtained by conditional measurements. However, it seems that very difficult implementations are expected. Nonlinear optical effects, from photon detection mechanisms to the use of nonlinear crystals may contribute positively towards construction of universal optical gates for QC. Parallelism provided by simultaneous operation of a gate at several wavelengths is a positive factor for quantum optics. Miniaturization of optical systems is possible and one implementation is discussed ahead. Scalability may the main obstacle in the path to quantum computation. It is important to identify possible ways to achieve scalability in the linear optics range. In this work a few sufficient requirements for a photon source are shown that could allow scalability for QC.

This work studies a three-bit optical network for implementation of a quantum half-adder. The states to be utilized were theoretically predicted in [5] and experimentally demonstrated by [6–8]. In these states, *each* photon is characterized by a polarization index p, a space index s, orbital angular momentum (OAM) index m and wavelength λ. Given the two possibilities for the indexes $p=0,1$ $(\rightarrow H,V)$ for horizontal and vertical polarizations, $s=0,1$ for two distinct trajectories, and $m=0,1$ $(\rightarrow n,l-n)$ for a photon pair carrying orbital angular momentum l, each photon represents three possible distinct bits. The association of just two bits $m=0,1$ to possible states with OAM n and $l-n$ is sufficient for the present work. It also fulfils the sum rule for the signal and idler photons where these two OAM values, where n is an arbitrary value, have to add to the converted pump photon OAM l [5]. These three bits (p,s,m or b_1,b_2,b_3) will provide 2^3 possible states $|psn\rangle$ for this single photon; they are going to be identified as the "input" to the quantum gates. Gate operation fulfills the truth table of a half-adder *plus* the carry operation for *each* bit. Parallel bit operation can also be performed with wavelengths $\lambda_1,\lambda_2,\ldots,\lambda_N$, within a selected time window $\Delta t \sim 1/\Delta\omega$ ($\Delta\omega$ being the down-conversion bandwidth).

A bright source of photon pairs or on-demand pairs is not impossible in principle and experimental results have demonstrated photon pairs and pair of pairs (see, for example, Ref. [9]). However, these sources present low efficiency and there is no procedure to separate contributions from a single pair, double pairs, and so on, from high-order emissions. This is still an unsolved problem but study of scalability conditions may point tracks to be followed.

II. HALF-ADDER

Figure 1 (left) shows a classical half-adder built from a Toffoli gate followed by a controlled-NOT (CNOT) gate. See Fig. 4.8 in Ref. [1] for an example of a Toffoli gate, and Ref. [10] for a possible CNOT implementation adequate for the present work. This classical circuit provides the truth table

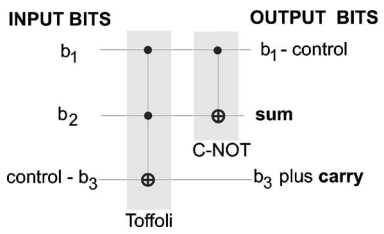

b_1	b_2	sum	carry
1	1	0	1
1	0	1	0
0	1	1	0
0	0	0	0

FIG. 1. (Left) Classical adder made from a Toffoli plus a CNOT gate. The input port labeled control can be also identified as ancilla port. (Right) Truth table for a half-adder.

*E-mail address: g-barbosa@northwestern.edu

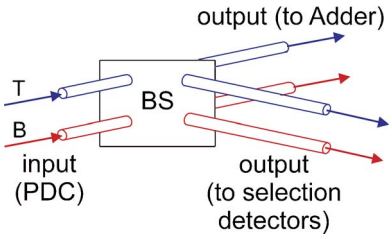

FIG. 2. (Color online) The beam splitter (BS), followed by angular momentum mask and detectors, constitute the selector that defines the wave state to input the gates.

given in Fig. 1 (right). The Toffoli gate discussed utilizes a C^2 gate where two bits *one* $(b_1=1, b_2=1)$ activates the interaction over the input third bit (b_3). Although operations of the half-adder are well defined, specific input bits used in this work with quantum sources are nondeterministic. Therefore, variations in photon source efficiency are simply translated into a slower or faster process. Spontaneous parametric down-conversion sources (SPDC) producing multiple pairs will be considered to show the scalability conditions. Either type I or type II processes could be utilized for the quantum adder, with small adaptations in the physical gate design. Type II SPDC will be assumed and provides the reader with an example of a CNOT gate recently demonstrated [10]. Entanglement of type II down-converted photons with orbital angular momentum l produce states of the form

$$|\Psi\rangle = \sum_{n=0}^{l} [|psn\rangle_{signal}|(1-p)(1-s)(l-n)\rangle_{idler} + |(1-p)(1-s)(l-n)\rangle_{signal}|psn\rangle_{idler}]. \quad (1)$$

A generic input to the adder is the product state

$$|\psi_{in}\rangle = |psn\rangle_{signal}|(1-p)(1-s)(l-n)\rangle_{idler} \otimes |\psi_{ancilla}\rangle.$$

Specific p,s,n values will be selected by detection of one photon in the pair. $|\psi_{ancilla}\rangle$ will be discussed ahead and should possibly be produced by the same source to fulfill scalability conditions. There are two possibilities for p, either H or V, and two space tags, say, T (top) or B (bottom) and two possible arbitrary values to the orbital angular momentum for signal and idler, n and $l-n$, constrained that these two values add to l (regardless the n value).

The $|\psi_{in}\rangle$ input down converted light can be sent to a beam splitter (BS) as shown in Fig. 2. At one port detectors preceded by polarizers (H or V) and an OAM mask for momentum m, select *one* photon with indexes p,s,m,λ (assume degenerate case with λ). Due to the entanglement, the input to the adder is given by the complementary values $1-p, 1-s, 1-m, \lambda$.

The linearity of optics allows simultaneous gate operation for N bits. The input to the adder can be represented by the state given by the classical-like vectorial product of binary vectors

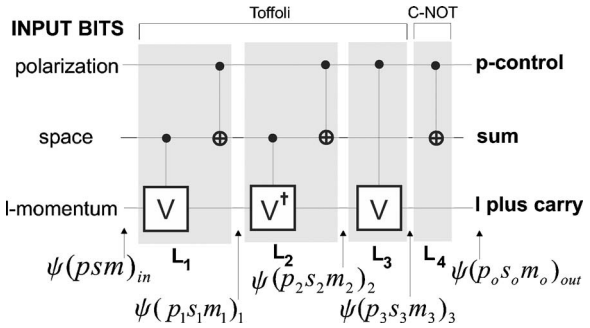

FIG. 3. Half-adder parts, constituted of a Toffoli gate followed by a CNOT gate. The Toffoli gate considered [1] is built with CNOT gates and interactions given by $V=(1-i)(I+i\sigma_X)/2$. The Adder will build from four physical blocks indicated as L_1, L_2, L_3, and L_4. Each block output provides the input to the following block. Modification of the wave function as the photon propagates through loops is indicated.

$$|psn\rangle_{signal} \rightarrow \psi(psm)_{in} = \begin{pmatrix} 1-p \\ p \end{pmatrix} \otimes \begin{pmatrix} 1-s \\ s \end{pmatrix} \otimes \begin{pmatrix} 1-m \\ m \end{pmatrix}, \quad (2)$$

with $m=0$ $(\rightarrow n)$ and $m=1$ $(\rightarrow l-n)$. This way a specific wave state $\psi(psm)_{in}$ defines the input to the gates shown in Fig. 2. The values (p,s) in this state define the bits to be summed and m is the control bit for the carry operation. Figure 3 is another representation of Fig. 1 adequate for this work. One should observe that the gate "wires" in Fig. 1 are abstract ones and that a given trajectory (specified by $s=0,1$) also carries the polarization and the angular momentum properties associated to the remaining "wire inputs." The Hilbert space of wave functions associated with $\psi(psm)_{in}$ is given by all possible combinations of p,s,m. Figure 4 shows all the blocks that constitute the half-adder. The BS at the input was described in Fig. 2. A physical depiction of the first loop (L_1) is shown in Fig. 5. After the input PBS, top and bottom inputs go clockwise or counterclockwise depending on the incoming polarization. H-polarized light goes clockwise and V-polarized light goes counterclockwise. The Dove prism inclined at $\varphi=45°$ directs clockwise or counterclockwise light into right and left beams. The central PBS in L_1, together with the beam splitters BS and the phase shifter will produce superposition of the ancilla photons with the PDC photon from the main input. These operations provide the interaction operator $V=(1-i)(I+i\sigma_X)/2$. Observing that the V action takes place at the orbital momentum space, it gives

$$V\begin{pmatrix} 1-m \\ m \end{pmatrix} = \frac{(1-i)}{2}(I+i\sigma_X)\begin{pmatrix} 1-m \\ m \end{pmatrix} = \frac{(1-i)}{2}\left[\begin{pmatrix} 1-m \\ m \end{pmatrix} + i\begin{pmatrix} m \\ 1-m \end{pmatrix}\right], \quad (3)$$

that gives a superposition of a mode m (or $l-m$) with $l-m$ (or m) with relative and overall phases. L_1 describes a V plus a CNOT gate (see Fig. 5). The V operation applied to $\psi(psm)_{in}$ is

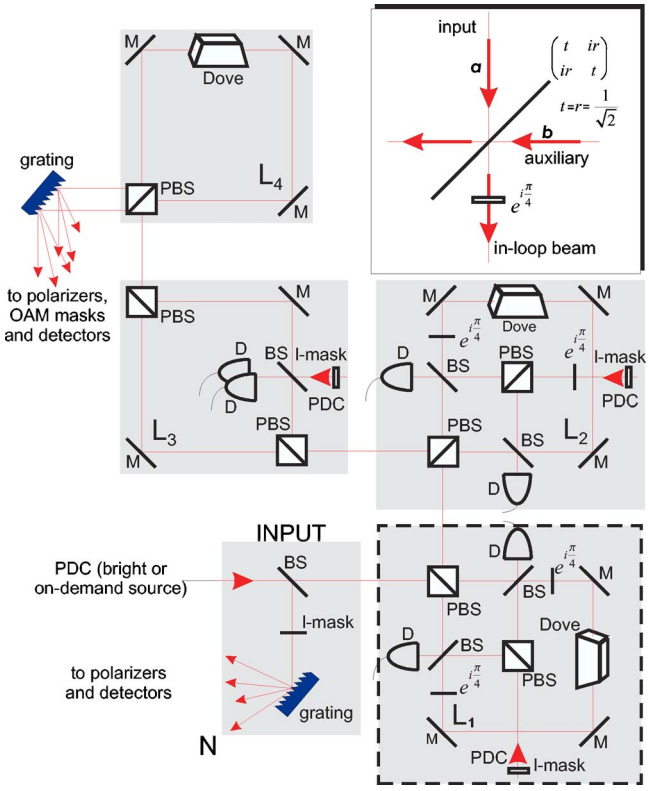

FIG. 4. (Color online) A block sketch of the half-adder. L_1 to L_3 constitute the Toffoli gate while L_4 is the CNOT gate. The arrows indicate PDC inputs. The inset shows the V interaction performed by action of a symmetric beam splitter BS on the SPDC photons from in-loop beam and auxiliary beams, followed by a phase shift of $e^{i\pi/4}$.

$$V|\psi_{in}\rangle = \begin{pmatrix} 1-p \\ p \end{pmatrix} \otimes \begin{pmatrix} 1-s \\ s \end{pmatrix} \otimes [sV + (1-s)I] \begin{pmatrix} 1-m \\ m \end{pmatrix}. \tag{4}$$

The CNOT operation (CN) acting on this wave state gives CN $V\psi(psm)_{in} = \psi(p_1 s_1 m_1)_1$, where

$$\begin{aligned} \psi(p_1 s_1 m_1)_1 &= \begin{pmatrix} 1-p \\ p \end{pmatrix} \otimes [p\sigma_X + (1-p)I] \\ &\times \begin{pmatrix} 1-s \\ s \end{pmatrix} \otimes [sV + (1-s)I] \begin{pmatrix} 1-m \\ m \end{pmatrix} \\ &= \begin{pmatrix} 1-p_1 \\ p_1 \end{pmatrix} \otimes \begin{pmatrix} 1-s_1 \\ s_1 \end{pmatrix} \otimes \left[\begin{pmatrix} 1-m \\ m \end{pmatrix} \right. \\ &+ \left. \frac{1+i}{2} \begin{pmatrix} s(-1+2m) \\ -s(-1+2m) \end{pmatrix} \right], \end{aligned} \tag{5}$$

where $p_1 = p$, $s_1 = p+s-2ps$, and there is no real m_1 value but a superposition state. However, the final output tags after L_4 have to be real and unique (loop 1 is developed in the Appendix with a standard ket wave-function notation to show consistent results in both formulations). A step-by-step similar calculation for wave states shown in Fig. 3 will give, successively, $p_2 = p$, $s_2 = s$, and m_2 in a superposition mode; $p_3 = p$, $s_3 = ps$, and $m_3 = ps+m-2psm$; and finally $p_o = p$, $s_o = p+s-2ps$, $m_o = ps+m-2psm$.

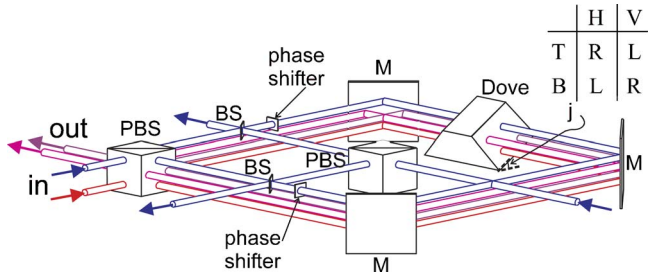

FIG. 5. (Color online) Loop 1: The input PBS is also the output element for L_1. The top and bottom inputs are shown as well as the right and left outputs. PBS splits horizontally polarized light into a clockwise direction in L_1 and vertically polarized light into a counterclockwise direction. The Dove prism inclined at $\varphi = 45°$ keeps the beam directions parallel but turns the top and bottom inputs into right and left outputs according to the table shown at the top right.

The vector exchange between a PDC input photon and an ancilla photon by the BS inside the loops represents an orbital angular momentum swap replacing mode m (or $l-m$), say, by $l-m$ (or m). The optical loops are designed so that the incoming PDC photons from each *input* became path indistinguishable from the ancilla photons in loops 1–3.

An electronic circuitry records the obtained counts and coincidences obtained. The interaction V acts on the subspace of OAM values and specifies the wave state at the block output. The inset of Fig. 4 shows the physical action of elements BS and phase shifter on incoming modes a and b. A symmetric beam splitter BS is represented with transmissivity $t = 1/\sqrt{2} = r$ and the phase shifter produces a phase shift of $e^{i\pi/4}$ for the output beam in the loop. The annihilation operator for this beam can be written $(1/\sqrt{2})(a+ib)$ (vacuum excluded). To transform the coefficient $(1/\sqrt{2})$ onto $(1-i)/2$ necessary for the V operation, see Eq. (3), one should apply $(1-i)/\sqrt{2} = e^{i\pi/4}$ to the BS output. This way, the V operation is performed by the BS and the phase shift imposed.

III. DETECTION

PBS at the output followed by a diffraction grating select incoming polarized light states. These states can be further selected by position and angular momentum values with appropriate masks. Detectors [or charge-coupled device (CCD) arrays] collect the transmitted light. At every sent signal of the form $\psi(psm)_{in}$ given in Eq. (2), it is easy to see that a detector should fire indicating the signal received, as given by $\psi(p_o s_o m_o)_{out}$. Therefore, the half-adder operations given by $\psi(psm)_{out} = \psi(p_0 s_0 m_0)_{out} = \text{H.a.} \times \psi(psm)_{in}$, fulfill the truth table in Fig. 1 that includes the carry operation.

IV. CIRCUIT CONSTRUCTION AND SOURCES

A. Miniaturization

Despite apparent complexity the half-adder blocks are very similar in construction and, as such, are convenient for miniaturization. Operation of the optical gates can be made

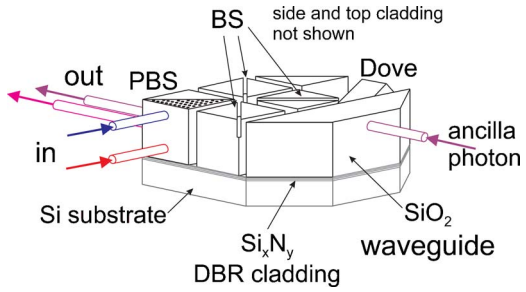

FIG. 6. (Color online) Loop 1 miniature is sketched. It consists of a Si substrate followed by a Si_xN_y distributed Bragg grating (DBG) and the miniature SiO_2 oxide optical waveguide. The top and side DBGs are not shown. x and y are chosen to allow a good refraction index difference between Si_xN_y and SiO_2 at the desired wavelength (e.g., 702 nm). The loop can be made smaller than 1 mm/side. Layers can also be separated by DBGs.

simultaneously with multiple wavelengths within a time window $\Delta t \sim 1/\Delta\omega$. This allows the parallel use of the quantum adder by using wavelength multiplexing before the input and output detectors. Miniaturization of loop 1 is sketched in Fig. 6. SiO_2 on Si_xN_y photonic cladding is described in [11].

Output from the half-adder may be used to input other optical circuits for further steps of optical computation. For example, use of a dynamical beam splitter switch could provide sequential operations with the same set of loops: light from the output of the half-adder may be redirected to its input by a variable transparency switch (nonlinear devices). This may form an optical feedback circuitry for multibit processing with the same half-adder module. On the other hand, much simpler classical architectures can be exploited for operations on this optical circuitry. For example, signals from detection of the sum and carry can prepare the input for another sum-carry step starting from the less significative bit to the more significative bit. The obtained less significative carry is now added to the subsequent more significative sum obtained and so on. This way a multibit summation can be obtained by exploiting the parallel wavelength multiplexing and the same optical circuitry. Therefore, simple quantum processors could be built and classical circuitries could also be used at the detection end of a processor. Several possibilities could be exploited for practical use of these optical circuits.

B. Photon sources

All of the described possibilities rely on the existence of photon sources able to generate multiple conjugated photons. These sources have to present physical separability for these photons so that they could input the different loops with the necessary time synchronism. The development of these sources may possibly utilize a poled periodic nonlinear structure (PPNL), Bragg distributed reflectors within a nonlinear medium, and other ideas to increase efficiency. Another question is if a source providing multiple conjugated photons such as the ones used in the quantum adder could also lead to a scalable system. This is a necessary condition to avoid the exponential growth of physical resources in the limit of a very large number of bits treated.

V. SCALABILITY

The use of a strong pulsed pump that leads to higher-order parametric processes is a candidate for this gate operation: Whenever spontaneous photons are generated but the medium is still excited, an stimulated emission process will follow. Stimulated emission contains a much larger number of photons and may provide the high flux or bright source necessary. In principle, a q-order process could generate q identical signals and q conjugated identical idlers. An example of this type of process with $q=2$ has been shown by [9] generating a four-photon state. Pumping a PPNL crystal with a strong pump laser with OAM is a candidate for this process. However, geometries that could lead to separability of the different q-order emissions have yet to be engineered.

As a starting assumption, assume that q identical signal photons and q idlers can be simultaneously generated and separately routed to the gate circuitry (preparation stage). E.g., for the loop L_1 discussed $q=2$. Considering *psm* degrees of freedom, this gives a total number of modes $M=q\times 2^3$ for signals and idlers. The number of photons is $n_p=2q$. Writing $n_p=\mu M$, this gives $\mu=1/2^2$. The associated Hilbert-space 2^N (N qubits) necessary for a process with a large number of M modes and n_p photons is given by [12]. It starts estimating the Hilbert-space dimension 2^N necessary to operate on n_T elementary processes given by the tensor product of their actions ($A=\Delta p\Delta q$) divided by the Planck constant $\hbar$,

$$2^N \sim \prod_{i=1}^{n_T} \frac{\Delta p_i \Delta q_i}{\hbar} = \frac{\prod_{i=1}^{n_T} \Delta p_i \Delta q_i}{\hbar^{n_T}}. \tag{6}$$

Equation (6) constrains N and n_T. Another step [12] is to use the Hilbert-space dimension for n_p photons occupying M modes

$$\Omega = \frac{(M+n_p-1)!}{(M-1)\,!\,(n_p)!}. \tag{7}$$

Comparing Eqs. (6) and (7) and making a Stirling expansion for large numbers, one obtains

$$2^N = \frac{(M+n_p-1)!}{(M-1)\,!\,(n_p)!} \simeq \frac{1}{\sqrt{2\pi}}(1+\mu)^M\left(1+\frac{1}{\mu}\right)^{n_p} \to \left(1+\frac{1}{\mu}\right)^{n_p}. \tag{8}$$

Therefore, $n_p=N/\log_2[1+(1/\mu)]$ and $M=N/\{\mu\log_2[1+(1/\mu)]\}$. This assures that n_p and M grow linearly with N and the process *is* scalable. Construction of a light source providing a multiple photon output as described in this section would lead to scalable optical systems adequate for quantum computation.

VI. CONCLUSIONS

A linear optics quantum multibit half-adder has been discussed using as a photon source PDC light from high-order emissions. These photons are entangled in polarization, en-

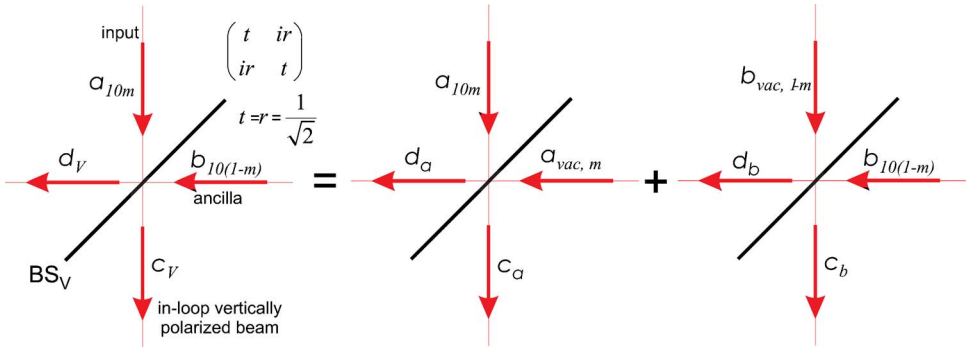

FIG. 7. (Color online) The figure at left shows the symmetric beam splitter BS_V with the incoming modes a_{10m} and $b_{10,1-m}$. The output beams are c_V and d_V. At the right-hand side BS_H is decomposed onto two beam splitters, one for each incoming mode, such that $c_V=c_a+c_b$ and $d_V=d_a+d_b$. A similar procedure is applied for the horizontally polarized photons at the beam splitter BS_V, giving c_H and d_H.

ergy, space, and orbital angular momentum. It was shown that given a proper light source (high-order PDC emissions) the half-adder fulfills the truth table giving sum plus carry. The assumed conditions indicate that development of an appropriate photon source leads to scalability conditions for operation with a high number of bits without the explosive need of physical resources. In this kind of system the resources grow linearly with the number of bits.

ACKNOWLEDGMENT

This work was supported by the U. S. Army Research Office Multidisciplinary University Research Initiative Grant No. W911NF-05-1-0197.

APPENDIX: LIGHT STATE OUTPUT FROM L_1

This Appendix just shows consistency of the result obtained in Eq. (5) with a pure quantum-mechanical calculation. Assume that an input photon, tagged by (spm) entering the PBS will arrive with one ancilla photon at the indicated BSs simultaneously. The indexes (spm) are determined by the selector detectors placed after the beam splitter BS before the input PBS. The ancilla photons are conjugated photon pairs, vertically or horizontally polarized, carrying orbital angular momentum $1-m$ (the notation $1-m$ just implies the complementary value to m. For a pump beam with orbital angular momentum l, "$1-m$" in fact implies the physical condition "$l-m$"). Writing the annihilation operators for the input photons as a_{psm} and for the ancilla photons $b_{p's'(1-m)}$ one may write the light state right in after the PBS together with the ancilla photon. The index $s=0$ means the top layer and $s=1$ the bottom layer while $p=0$ designates horizontally polarized light and $p=1$ vertically polarized light. The wave state for the input and ancilla photon can be written as

$$\begin{aligned} &O^{PBS}|psn\rangle \otimes |ancilla\rangle \\ &\quad \equiv O^{PBS}|\Psi_{psm}\rangle = [\delta_{s1}(-i\delta_{p1}a^{\dagger}_{11m} + \delta_{p0}a^{\dagger}_{01m}) \\ &\qquad + (\delta_{s0}/\sqrt{2})(\delta_{p0}a^{\dagger}_{00m}b^{\dagger}_{00(1-m)} - \delta_{p1}a^{\dagger}_{10m}b^{\dagger}_{10(1-m)})]|0\rangle. \end{aligned} \tag{9}$$

The δ_{s1} term is related to the bottom layer and δ_{s0} to the top layer. After a short propagation a vertically polarized photon going counterclockwise in L_1 reach BS_V while a horizontally polarized photon will propagate in a clockwise direction and will reach BS_H. PBS action is sketched in Fig. 7. Extracting operators to replace into the input wave state one obtains the beam splitter operations O^{BS_V} and O^{BS_H} on this wave state. The Dove prism operation is indicated at the right corner of Fig. 5. Assuming that one of the detectors in L_1 would fire with a single photon, one should write the output wave state $|\widetilde{\Psi_{psm}}\rangle_1$, after PBS,

$$\begin{aligned} |\widetilde{\Psi_{psm}}\rangle_1 &= [I - |1_{d_V}\rangle\langle 1_{d_V}|][I - |1_{d_H}\rangle\langle 1_{d_H}|]|\Psi_{psm}\rangle_1 \\ &= \Bigg[\delta_{s1}(\delta_{p1}a^{\dagger}_{11m} + \delta_{p0}a^{\dagger}_{01m}) \\ &\quad + \frac{\delta_{s0}}{\sqrt{2}}\Bigg(-\frac{\delta_{p0}}{2}[-i(d^{\dagger}_H d^{\dagger}_H + c^{\dagger}_H c^{\dagger}_H) + \sqrt{2}c^{\dagger}_H a^{\dagger}_{vac,m} \\ &\quad + i\sqrt{2}c^{\dagger}_H b^{\dagger}_{vac,1-m} - 2b^{\dagger}_{vac,1-m}a^{\dagger}_{vac,m}] \\ &\quad - i\frac{\delta_{p1}}{2}[d^{\dagger}_V d^{\dagger}_V - c^{\dagger}_V c^{\dagger}_V + i\sqrt{2}c^{\dagger}_V b^{\dagger}_{vac,1-m} \\ &\quad + \sqrt{2}c^{\dagger}_V a^{\dagger}_{vac,m} - 2ib^{\dagger}_{vac,1-m}a^{\dagger}_{vac,m}] \Bigg) \Bigg] |0\rangle. \end{aligned} \tag{10}$$

With the wave state (10) the output photon number from L_1 can be calculated and one obtains

$$\begin{aligned} \langle\widetilde{\Psi_{psm}}|c^{\dagger}_V c_V|\widetilde{\Psi_{psm}}\rangle &= \delta_{s0}\delta_{p1}, \\ \langle\widetilde{\Psi_{psm}}|c^{\dagger}_H c_H|\widetilde{\Psi_{psm}}\rangle &= \delta_{s0}\delta_{p0}, \\ \langle\widetilde{\Psi_{psm}}|a^{\dagger}_{01m}a_{01m}|\widetilde{\Psi_{psm}}\rangle &= \delta_{s1}\delta_{p0}, \\ \langle\widetilde{\Psi_{psm}}|a^{\dagger}_{11m}a_{11m}|\widetilde{\Psi_{psm}}\rangle &= \delta_{s1}\delta_{p1}. \end{aligned} \tag{11}$$

Inspection shows that this output gives the results calculated in Eq. (5), namely $p_1=p$, $s_1=p+s-2ps$, and m_1 is a superposition of m and $1-m$ OAM states. Remaining loops can be treated similarly.

[1] For a comprehensive introduction, see M. A. Nielsen and I. L. Chuang, *Quantum Computation and Quantum Information* (Cambridge University Press, Cambridge, UK, 2000); A. Barenco *et al.*, Phys. Rev. A **52**, 3457 (1995); D. Bouwmeester, A. Ekert, and A. Zeilinger, *The Physics of Quantum Information* (Springer-Verlag, Berlin, 2000).

[2] N. A. Gershenfeld and I. L. Chuang, Science **275**, 350 (1997); M. D. Price, S. S. Somaroo, C. H. Tseng, J. C. Gore, A. F. Fahmy, T. F. Havel, and D. G. Cory, J. Magn. Reson. **140**, 371 (1999).

[3] Quantum Computing Program Review 2005, Tampa-Florida (Sponsored by: ARO, NSA, and ARDA) (unpublished).

[4] E. Knill, R. Laflamme, and G. J. Milburn, Nature (London) **409**, 4 (2001).

[5] H. H. Arnaut and G. A. Barbosa, Phys. Rev. Lett. **85**, 286 (2000); G. A. Barbosa and H. H. Arnaut, Phys. Rev. A **65**, 053801 (2002); G. A. Barbosa, Eur. Phys. J. D **22**, 433 (2003).

[6] A. Mair, A. Vaziri, G. Weihs, and A. Zeilinger, Nature (London) **412**, 313 (2001).

[7] A. R. Altman, K. G. Köprülü, E. Corndorf, P. Kumar, and G. A. Barbosa, Phys. Rev. Lett. **94**, 123601 (2005).

[8] J. T. Barreiro, N. K. Langford, N. A. Peters, and P. G. Kwiat, Phys. Rev. Lett. **95**, 260501 (2005).

[9] Z. Y. Ou, J.-K. Rhee, and L. J. Wang, Phys. Rev. Lett. **83**, 959 (1999).

[10] M. Fiorentino and F. N. C. Wong, Phys. Rev. Lett. **93**, 070502-1-4 (2004); see, also, J. L. O'Brien, G. J. Pryde, A. G. White, T. C. Ralph, and D. Branning, Nature (London) **426**, 264 (2003); T. B. Pittman, B. C. Jacobs, and J. D. Franson, Phys. Rev. Lett. **88**, 257902-1-4 (2002).

[11] Y. Yi, S. Akiyama, P. Bermel, X. Duan, and L. C. Kimerling, Opt. Express **12**, 477 (2004).

[12] R. Blume-Kohout, C. M. Caves, and I. H. Deutsch, Found. Phys. **32**, 1641 (2002).